Open Access
Baghdad Science Journal Vol.12(2)2015

# On The Nearby-Tip Strain Investigation and Failure-Propability Evaluation for Impacted Thin Plates Using the 2-Random-Variables Multi-Canonical-Based Joint Propability Distributions

*Rasha A. Ali** *Muthanna A. Ali***

Received 17, April, 2014
Accepted 22, June, 2014



## Abstract:

The study of the validity and probability of failure in solids and structures is highly considered as one of the most incredibly-highlighted study fields in many science and engineering applications, the design analysts must therefore seek to investigate the points where the failing strains may be occurred, the probabilities of which these strains can cause the existing cracks to propagate through the fractured medium considered, and thereafter the solutions by which the analysts can adopt the approachable techniques to reduce/arrest these propagating cracks.

In the present study a theoretical investigation upon simply-supported thin plates having surface cracks within their structure is to be accomplished, and the applied impact load to these thin plates tends to induce almost infinite strains nearby the crack tip of the existing cracks. The distribution of these strains and the probability distribution of failure due to these strains are to be of a particular importance within the current research.

Within the current study a modified theoretical technique, which is derived from the classical plate theory, whose concepts are illustrating the required plane-stress conditions for fractured thin plates, taking into consideration the impact-load effects in conjunction with the fracture-mechanics concepts, is to be followed and obeyed so as to arrive at the required equations representing the nearby-tip strains within the thin plates made from the pure aluminum 1100 type alloys. A further statistically-based analysis must lead into the utilization of the joint probability distributions having two random variables in order to construct the required probability distributions of the failure which may be occurred due to the highly-localized nearby-tip strains.

**Key words:** Joint Probability Distributions, Multi-Canonical Probability Functions, Nearby-Tip Strains, Thin Plates, Fracture and Failure Analyses.

## Introduction:

The present research aims to study the solid body, whose structure is experiencing large deformations and loss of contact between parts of the body itself, undergoing extreme loading which leads to the elastic-plastic deformation with or without the occurrence of total fracture. As a contributing fact, fracture may be evolved before, after, or in conjunction with the occurrence of large deformation process **[1]**. Of a particular interest within the current work is to illustrate , using the traditional constitutions of the classical plate theory **[2]**, the strains induced within the thin plates used, and to statistically investigate the joint probability distributions, the 2-random-variables-type special probability distributions, by which the induced strains may cause a total failure for the

* University of Baghdad– Physical Education College
** University of Baghdad - Department of Mechanical Engineering
Rasha.stat@gmail.com

plates used. The current study is to be accomplished to investigate the nearby-tip strain distributions and failing-strains probability distributions for variable crack length values (10, 20, and 30mm) and also for two types of plate aspect ratio (1 and 2) for the pure-aluminum-1100-type thin plates.

**D. S. Dugdale (1960) [3]** has investigated the yielding undergone at the end of a surface or through (internal) slit in a sheet by an external load, and obtained a relation between the extent of the plastic yielding and the external load applied. To verify this relation, panels containing internal and edge slits were loaded in tension and lengths of plastic zones were measured. The elastic stress intensity factors are normalized dynamically for ductile materials into elastoplastic stress intensity factors, in order to distinguish how much stresses and strains near the crack tip and speeds of the propagating cracks for an elastic-ideally plastic Tresca material which is experiencing an external load.

Hamid Ahmadi and Mohammad Ali Lotfollahi-Yaghin **(2012) [4]** proposed that the stress concentration factor (SCF) is one of the most important parameters in the fatigue reliability analysis of steel offshore structures. This parameter exhibits considerable scatter which calls for greater emphasis in accurately computing the SCFs for predicting the fatigue life of these structures. As far as the authors are aware, no comprehensive research has been carried out on the probability distribution of SCFs in tubular joints, especially multi-planar ones, which cover the majority of practical applications. What has been used so far as the probability distribution of SCFs in the reliability analysis of offshore structures is mainly based on assumptions and limited observations, especially in terms of distribution parameters. In the present paper, results of performing finite element (FE) analysis on 81 steel multi-planar dual-kit-tubular (DKT) joints have been used to propose a probability distribution model for SCFs along the weld toe of the central brace under axial loads. Based on the multi-planar DKT-joint FE models which are verified against experimental results and the predictions of Lloyd's Register (LR) equations, a set of SCF sample databases was constructed. 15 different probability density functions (PDFs) were fitted to the relative frequency histograms of the SCF samples. The maximum likelihood method was used to determine the parameters of each distribution. Standard goodness-of-fit tests led to the conclusion that the Inverse Gaussian distribution is the best probability model for the peripheral distribution of SCFs along the weld toe and the Birnbaum–Saunders distribution is the best one for the maximum value of weld toe SCF.

D. Yevick **(2003) [5]** has adapted multicanonical evaluation sampling to the evaluation of general probability distribution functions such as those appearing in communication system modeling. This letter also demonstrates that joint probability distributions can be computed in an identical manner. To illustrate, one may determine the joint distribution function between the first- and second-order polarization-mode dispersion in an optical fiber.

## Analytical Approach:

### 1. Nearby-Tip Strain Distribution Evaluation:

The mathematical model of a cracked thin plate is shown in Fig. (1), the following underlying assumptions are adequately convenient to be utilized in order to arrive at the final analytical expressions: the plate is thin enough for plane stress to occur,

isothermal conditions are assumed for the linearly isotropic continuum, i.e., any temperature change during the impact process is of no concern within the present illustration, and the impacted-plate alloy type is homogenous and of a linearly-elastic-ideally-plastic behavior whose yield limit can be approximated, with fairly good results, by Tresca's failure criterion. Hence, proceeding from the plane-stress-based equilibrium equations for a solid medium, small-strain-theory-based kinematic constraints, for-linearly-isotropic-alloy-type Hooke's law, and from the assumed Airy's stress function relations **[1]**

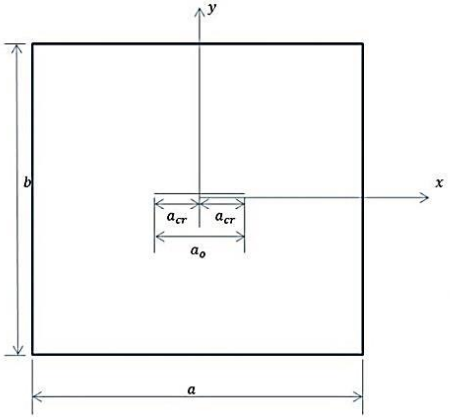


**Fig. (1) The Mathematical Model of a Centrally-Cracked Plate**

one can arrive at the following bi-potential equation

$$\nabla^2(\nabla^2\Omega) = 0 \quad \dots\dots\dots (1)$$

whose general solution, achieved by Mushelishvilli **[2]**, is given by

$$\Omega = \frac{1}{2} Re[\bar{z}\Phi(z) + \Psi(z)] \quad \dots\dots\dots (2)$$

where $\Phi(z)$ and $\Psi(z)$ are arbitrarily-introduced analytic functions, the second derivative of $\Omega$ with respect to $x$ and/or $y$ may give

$$\sigma_{xx} = \frac{\partial^2\Omega}{\partial y^2} = Re\left(\bar{\Phi} - \frac{\bar{z}\bar{\Phi} + \bar{\Psi}}{2}\right)$$
$$\sigma_{yy} = \frac{\partial^2\Omega}{\partial x^2} = \left(\bar{\Phi} + \frac{\bar{z}\bar{\Phi} + \bar{\Psi}}{2}\right) \quad \dots\dots\dots (3)$$
$$\tau_{xy} = -\frac{\partial^2\Omega}{\partial x \partial y} = Im\left(\frac{\bar{z}\bar{\Phi} + \bar{\Psi}}{2}\right)$$

In order to arrive at the displacements, we must invoke the peculiarities of linearly-isotropic material characteristics (Hooke's law) and the small-strain-theory-based kinematic constraints to (neglecting rigid-body terms emanated due to the translation and/or rotation of the rigid body) proceed into **[1][6]**

$$u_x = \frac{1}{4G} Re\left(\left(\frac{3-\nu}{1+\nu}\right)\Phi - \bar{z}\bar{\Phi} - \bar{\Psi}\right)$$
$$u_y = \frac{1}{4G} Im\left(\left(\frac{3-\nu}{1+\nu}\right)\Phi + \bar{z}\bar{\Phi} + \bar{\Psi}\right) \quad \dots\dots (4)$$

Westergaard **[7]** has figured out a relation between the two analytic functions $\Phi(z)$ and $\Psi(z)$ by imposing the boundary condition $\tau_{xy} = 0$ along $y = 0$, for cracks experiencing tension tractions (mode I cracking), so as to proceed into

$$\bar{\Psi} = -z\bar{\Phi} \quad \dots\dots\dots (5)$$

which may be substituted into eq. (3) and into eq. (4) in order to arrive at the following representation for predominant mode-I stresses and displacements

$$\sigma_{xx} = Re\bar{\Phi} - yIm\bar{\bar{\Phi}}$$
$$\sigma_{yy} = Re\bar{\Phi} + yIm\bar{\bar{\Phi}} \quad \dots\dots\dots (6)$$
$$\tau_{xy} = -yRe\bar{\bar{\Phi}}$$

$$u_x = \frac{1}{2G(1+\nu)} Re\Phi - yIm\bar{\Phi}$$
$$u_y = \frac{1}{G(1+\nu)} Im\Phi - yRe\bar{\Phi} \quad \dots\dots\dots (7)$$

By firstly solving for stresses and displacements in the vicinity of the crack tip (which lies at $x = a_{cr}$, $y = 0$) without any presence of traction stresses, and then imposing the traction stresses at $|x| < a_{cr}$, $y = 0$ in order to simulate the crack, Sedov **[8]** has pointed out a general solution for the analytic function $\Phi(z)$ concerning an infinite plate whose crack is having a length of $2a_{cr}$ (Fig. (1)), therefore, we have

$$\bar{\Phi}_I = \frac{1}{\pi\sqrt{z^2 - {a_{cr}}^2}} \int_{-a_{cr}}^{a_{cr}} \frac{\lambda_2(\xi)\sqrt{{a_{cr}}^2 - \xi^2}}{z - \xi} d\xi \quad \dots (8)$$

Studying the behavior of stresses and strains in the vicinity of the right-hand crack tip, ($z + a_{cr} \approx 2a_{cr}$, $z - \xi \approx a_{cr} - \xi$), introducing the traction $\sigma_{yy} = 0$ along $|x| < a_{cr} + c$ and superimposing the traction

$\sigma_{yy} = \sigma_Y$ along $a_{cr} < |x| < a_{cr} + c$ by utilizing the superposition principle (in accordance off Dugdale model **[3]** for elastoplastically-deformed thin plates), will yield the following relation of the analytic function

$$\bar{\Phi}_I = \frac{K_{I,ep}}{\sqrt{2\pi(z-a_{cr})}} = \frac{\sigma_Y\left[\sqrt{\pi\left(a_{cr}+\frac{a_o}{16}\left(\frac{\pi}{\sigma_Y}\right)^2\right)} - 2\sqrt{\frac{a_{cr}+\frac{a_o}{16}\left(\frac{\pi}{\sigma_Y}\right)^2}{\pi}}\sin^{-1}\left(\frac{a_{cr}}{a_{cr}+\frac{a_o}{16}\left(\frac{\pi}{\sigma_Y}\right)^2}\right)\right]}{\sqrt{2\pi(z-a_{cr})}} \quad \dots (9)$$

The introduction of notation $(z - a_{cr} = re^{i\theta})$ and the substitution of eq. (9) into eq. (7) will yield the following the required local elastic-plastic displacement fields for mode I

$$\begin{bmatrix} u_x \\ u_y \end{bmatrix}_{ep} = \frac{K_{I,ep}}{2G}\sqrt{\frac{r}{2\pi}}\left(\frac{3-\nu}{1+\nu} - \cos\theta\right)\begin{bmatrix} \cos\theta/2 \\ \sin\theta/2 \end{bmatrix} \dots\dots\dots (10)$$

$$\begin{bmatrix} u_x \\ u_y \end{bmatrix}_{ep} = \frac{\sigma_Y\left[\sqrt{\pi\left(a_{cr}+\frac{a_o}{16}\left(\frac{\pi}{\sigma_Y}\right)^2\right)} - 2\sqrt{\frac{a_{cr}+\frac{a_o}{16}\left(\frac{\pi}{\sigma_Y}\right)^2}{\pi}}\sin^{-1}\left(\frac{a_{cr}}{a_{cr}+\frac{a_o}{16}\left(\frac{\pi}{\sigma_Y}\right)^2}\right)\right]}{2G}\sqrt{\frac{r}{2\pi}}\left(\frac{3-\nu}{1+\nu} - \cos\theta\right)\begin{bmatrix} \cos\theta/2 \\ \sin\theta/2 \end{bmatrix} \dots\dots\dots\dots (11)$$

Whose constants $\nu$, $G$, and $\sigma_Y$ can be determined by using the following table for pure-aluminum-1100-alloy-type properties

| **Pure Aluminum 1100 Properties [9]** | |
|---|---|
| Poisson's Ratio $(\nu)$ | 0.334 |
| Young's Modulus $(E)$ | 69 $Gpa$ |
| Shear Modulus $(G)$ | 26 $Gpa$ |
| Yield Limit $(\sigma_Y)$ | 8 $Mpa$ |

A further approach that must be followed, by using the small-strain analysis, in order to determine the nearby-tip strain distribution, from which the failing-strains probability distributions can thereafter be recognized in the upcoming subsection. Now, one can therefore anticipate the following expression for the nearby-tip strain field

$$\begin{bmatrix} \varepsilon_{xx} \\ \varepsilon_{yy} \end{bmatrix}_{ep} = \begin{bmatrix} \frac{\Delta u_{x,ep}}{\Delta x} \\ \frac{\Delta u_{y,ep}}{\Delta y} \end{bmatrix} = \begin{bmatrix} d/dx \\ d/dy \end{bmatrix}\left[\frac{\sigma_Y}{2G}\left[\sqrt{\pi\left(a_{cr}+\frac{a_o}{16}\left(\frac{\pi}{\sigma_Y}\right)^2\right)} - 2\sqrt{\frac{a_{cr}+\frac{a_o}{16}\left(\frac{\pi}{\sigma_Y}\right)^2}{\pi}}\sin^{-1}\left(\frac{a_{cr}}{a_{cr}+\frac{a_o}{16}\left(\frac{\pi}{\sigma_Y}\right)^2}\right)\right]\right]\sqrt{\frac{r}{2\pi}}\left(\frac{3-\nu}{1+\nu} - \cos\theta\right)\begin{bmatrix} \cos\theta/2 \\ \sin\theta/2 \end{bmatrix} \dots\dots\dots (12)$$

## 2. Failing-Strains Probability Density Function Evaluation:

It is convenient from now on to illustrate the behavior that the nearby-tip strains (eq. 12) apt to cause the existing cracks to propagate through the plates considered, and this behavior is thereby significantly appropriate to illustrate the probability of the existing cracks to propagate due to the induced strains. In accordance to Fig. (2), the region enclosed by $-10 \ll X \ll 10$ and $0 \ll Y \ll 20$ can be divided into 1-mm-spacing gridpoints in which the nearby-tip strains and the failure probability distributions can be easily determined. Having known the region where the failing strains can act through the medium considered, the continuous-type multi-canonical joint probability density functions are thereby to be processed since the probability distribution is based on unaccountably-infinite-type random variables **[10]**. The evaluation process of the continuous-type multi-canonical 2-random-variables joint probability density functions is therefore given by **[5]**

$$P\left(\frac{\Theta(X)}{\Theta(X)+\Theta(Y)} = x = r\cos\theta\right) = \frac{d}{dx}\int_{x=-10}^{10}\frac{\psi(x)dx}{\psi(x)+\delta(y)} \quad \dots (13)$$

$$P\left(\frac{\Theta(Y)}{\Theta(X)+\Theta(Y)} = y = r\sin\theta\right) = \frac{d}{dy}\int_{y=0}^{20}\frac{\delta(y)dy}{\psi(x)+\delta(y)}$$

which can further be proceeded into

$$P(x)=\frac{d}{dx}\int_{x=-10}^{10} d/dx\left[\frac{\sigma_Y}{2G}\left[\sqrt{\pi\left(a_{cr}+\frac{a_o}{16}\left(\frac{\pi}{\sigma_Y}\right)^2\right)}-2\sqrt{\frac{a_{cr}+\frac{a_o}{16}\left(\frac{\pi}{\sigma_Y}\right)^2}{\pi}}\sin^{-1}\left(\frac{a_{cr}}{a_{cr}+\frac{a_o}{16}\left(\frac{\pi}{\sigma_Y}\right)^2}\right)\right]\sqrt{\frac{r}{2\pi}}\left(\frac{3-\nu}{1+\nu}-\cos\theta\right)\begin{bmatrix}\cos\theta/2\\ \sin\theta/2\end{bmatrix}dx$$

$$P(y)=\frac{d}{dy}\int_{y=0}^{20} d/dy\left[\frac{\sigma_Y}{2G}\left[\sqrt{\pi\left(a_{cr}+\frac{a_o}{16}\left(\frac{\pi}{\sigma_Y}\right)^2\right)}-2\sqrt{\frac{a_{cr}+\frac{a_o}{16}\left(\frac{\pi}{\sigma_Y}\right)^2}{\pi}}\sin^{-1}\left(\frac{a_{cr}}{a_{cr}+\frac{a_o}{16}\left(\frac{\pi}{\sigma_Y}\right)^2}\right)\right]\sqrt{\frac{r}{2\pi}}\left(\frac{3-\nu}{1+\nu}-\cos\theta\right)\begin{bmatrix}\cos\theta/2\\ \sin\theta/2\end{bmatrix}dy$$

...(14)

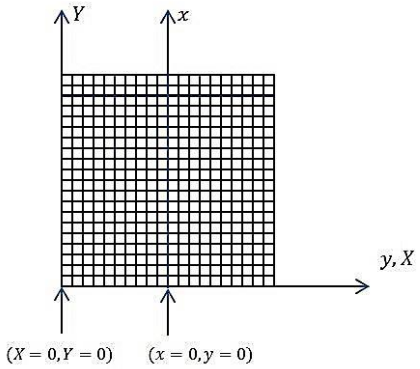


**Fig. (2) Transformation Process into the Random Variables *X* and *Y***

## Results and Discussion:

### 1. Nearby-Tip Strains

It has been previously demonstrated that the strains induced in the vicinity of the crack tip can be evaluated by using the eq. (12), now it is significantly appropriate to illustrate how intense these strains can be within the structure of the thin plates. By examining Fig. (3) to Fig. (14) the amount of the $X$-axis and $Y$-axis nearby-tip strains would exhibit an exponential decrease as the distance from the crack tip decreases, and the values of the maximum strains would therefore be always at the point where the crack tip lies at. It can also be demonstrated that the both $X$-axis and $Y$-axis nearby-tip strains would undergo 13.45% and 11.41% increase as the existing crack length within the thin plates increases from 10 mm to 20 mm and from 20 mm to 30 mm respectively. Likewise, the amount of the strains would exhibit 34.21% increase when the plate aspect ratio increases from 1 to 2. The low-aspect-ratio and short-crack-length thin plates would then be more legitimate to be utilized in the design purposes, in the sense that they experience lower nearby-tip strains than what is induced in the high-aspect-ratio and long-crack-length thin plates due to the impacting load.

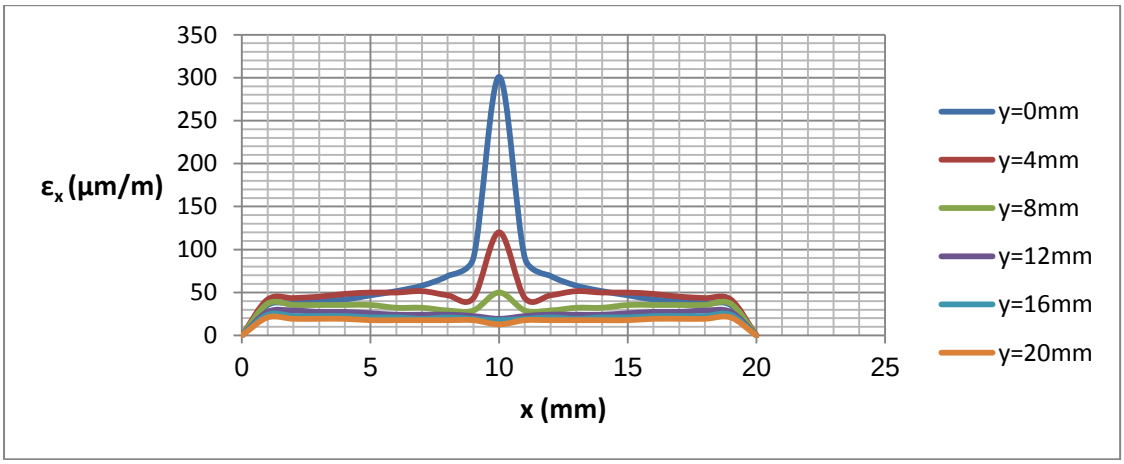


**Fig. (3) Nearby-Tip Strain Induced Towards the X-axis for *Aspect Ratio* = 2.000, and $a_o = 10mm$.**

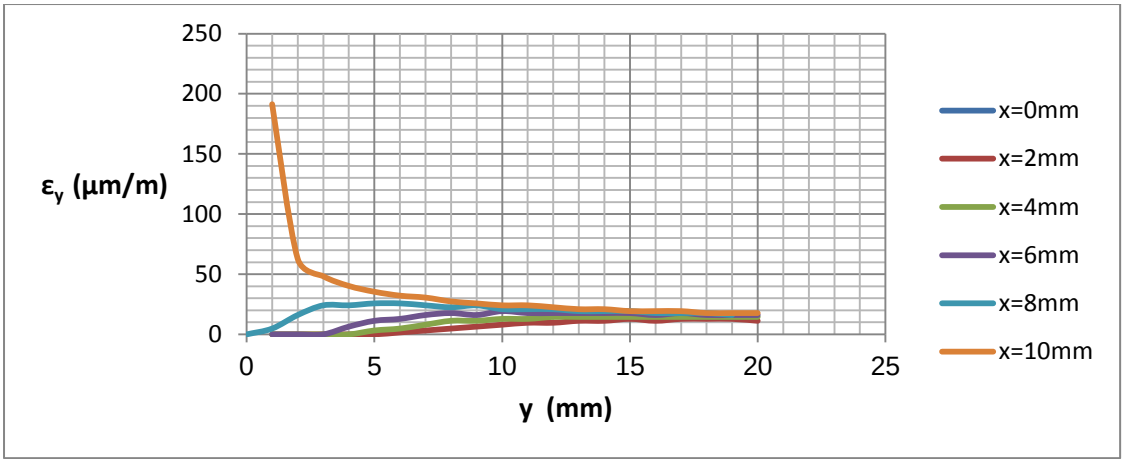


**Fig. (4) Nearby-Tip Strain Induced Towards the Y-axis for $Aspect\ Ratio = 2.000$, and $a_o = 10mm$.**

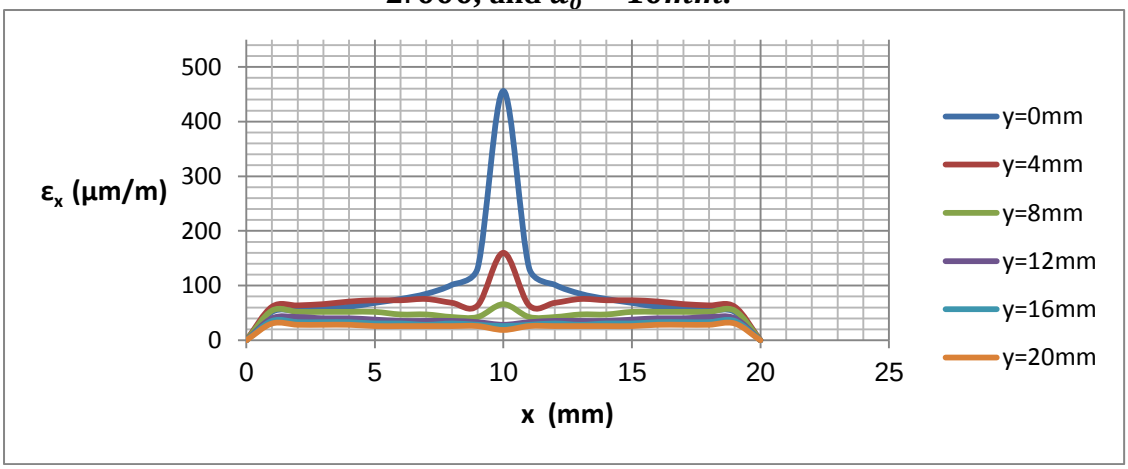


**Fig. (5) Nearby-Tip Strain Induced Towards the X-axis for $Aspect\ Ratio = 2.000$, and $a_o = 20mm$**

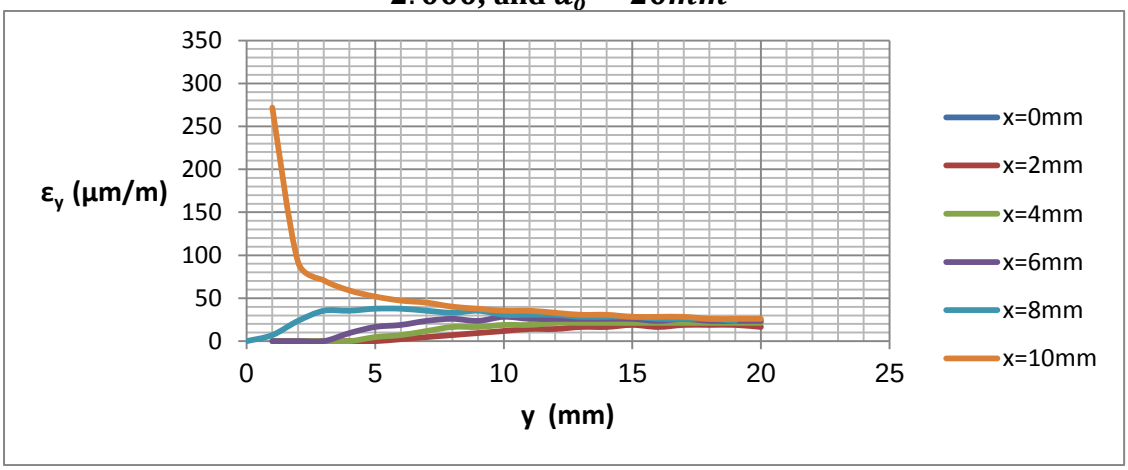


**Fig. (6) Nearby-Tip Strain Induced Towards the Y-axis for $Aspect\ Ratio = 2.000$, and $a_o = 20mm$.**

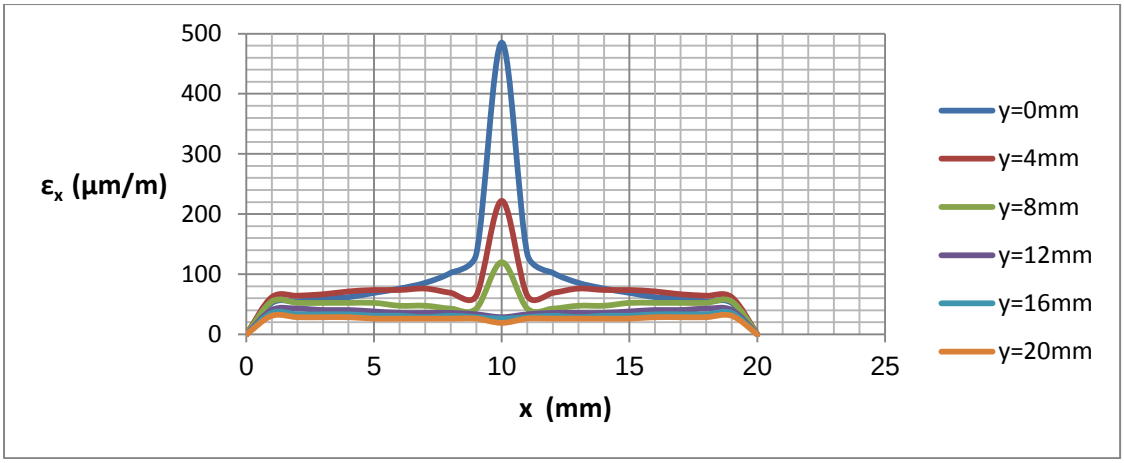


**Fig. (7) Nearby-Tip Strain Induced Towards the X-axis for $Aspect\ Ratio = 2.000$, and $a_o = 30mm$.**

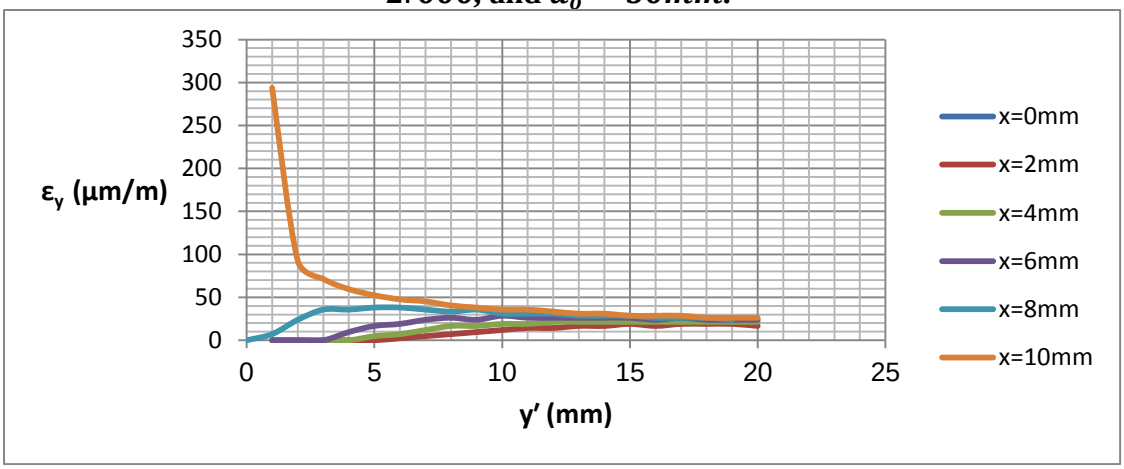


**Fig. (8) Nearby-Tip Strain Induced Towards the Y-axis for $Aspect\ Ratio = 2.000$, and $a_o = 30mm$.**

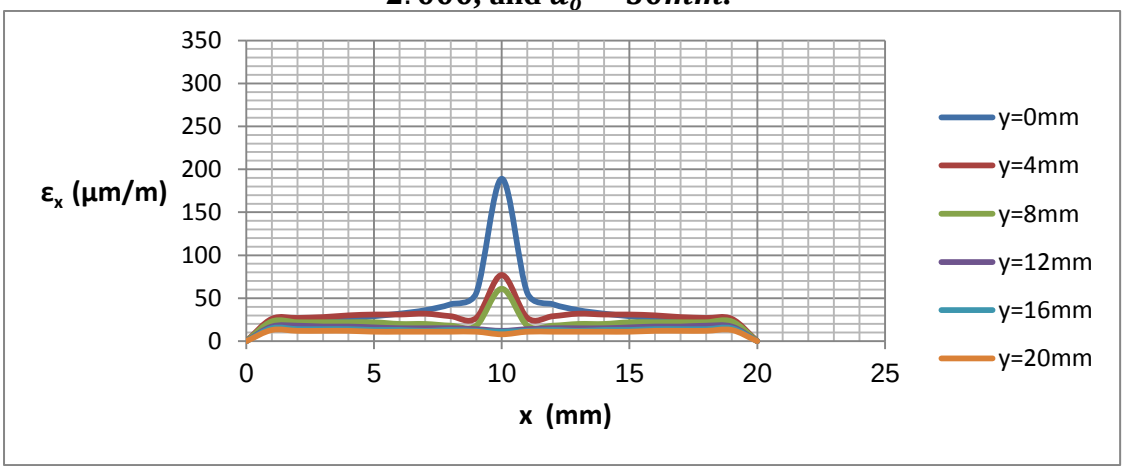


**Fig. (9) Nearby-Tip Strain Induced Towards the X-axis for $Aspect\ Ratio = 1.000$, and $a_o = 10mm$.**

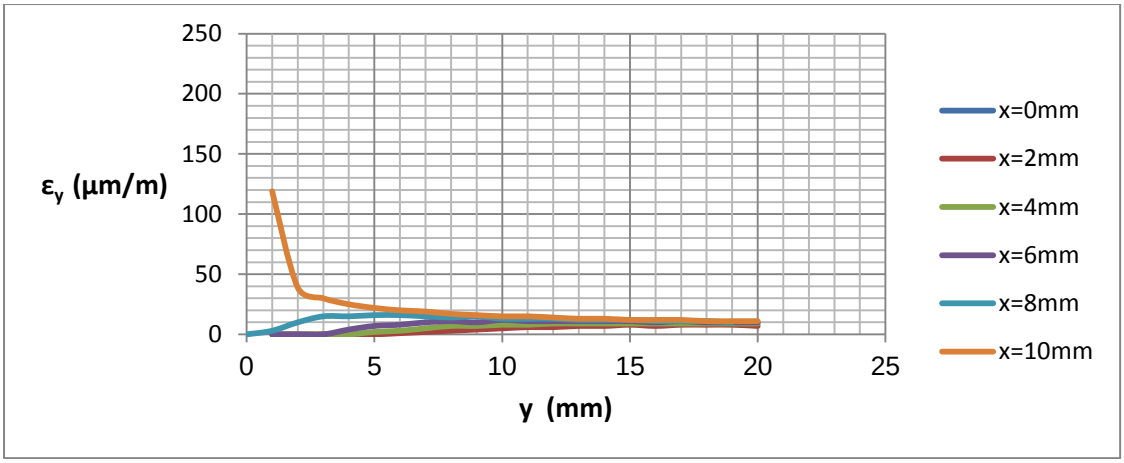


**Fig. (10) Nearby-Tip Strain Induced Towards the Y-axis for $Aspect\ Ratio = 1.000$, and $a_o = 10mm$.**

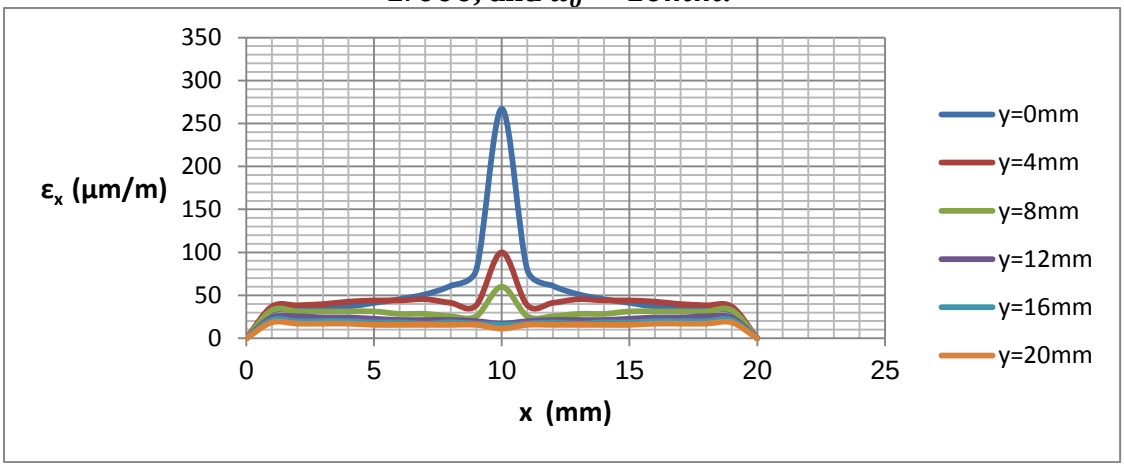


**Fig. (11) Nearby-Tip Strain Induced Towards the X-axis for $Aspect\ Ratio = 1.000$, and $a_o = 20mm$.**

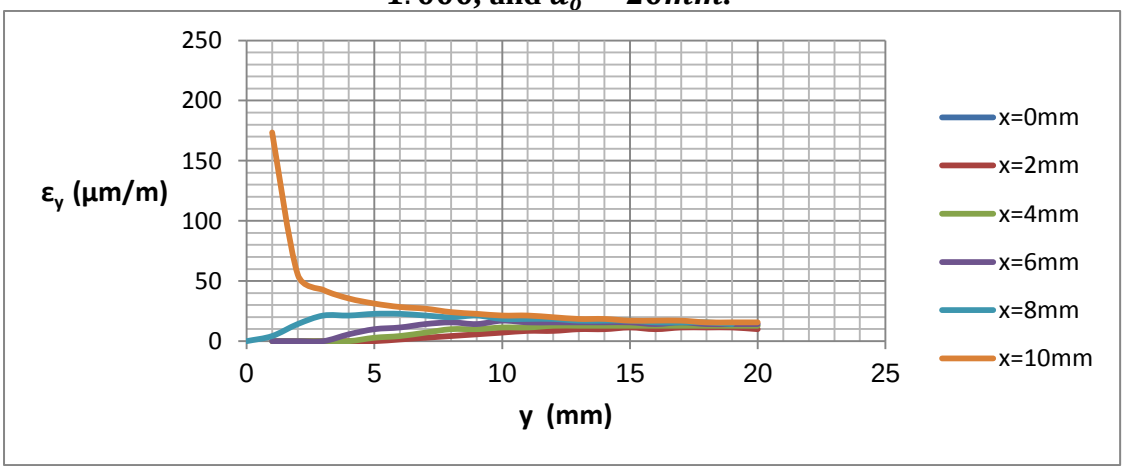


**Fig. (12) Nearby-Tip Strain Induced Towards the Y-axis for $Aspect\ Ratio = 1.000$, and $a_o = 20mm$.**

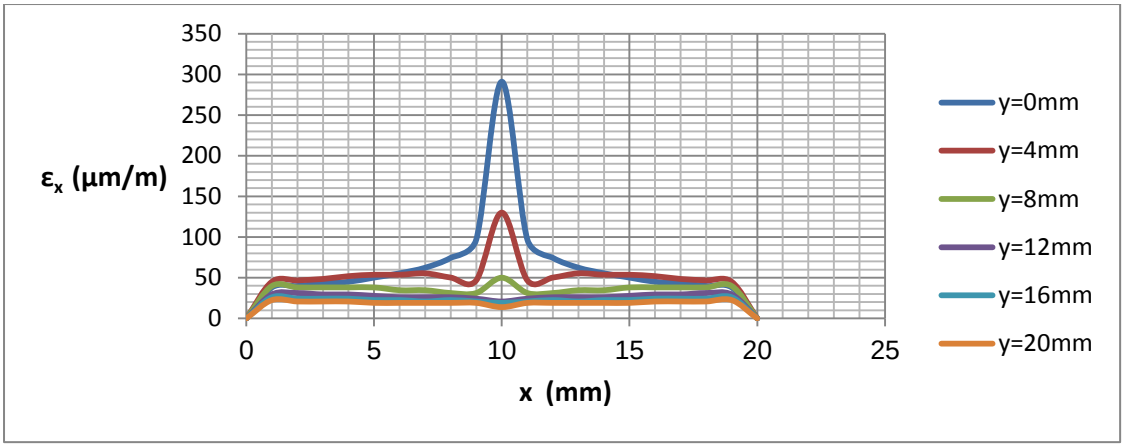


**Fig. (13) Nearby-Tip Strain Induced Towards the X-axis for $Aspect\ Ratio = 1.000$, and $a_o = 30mm$.**

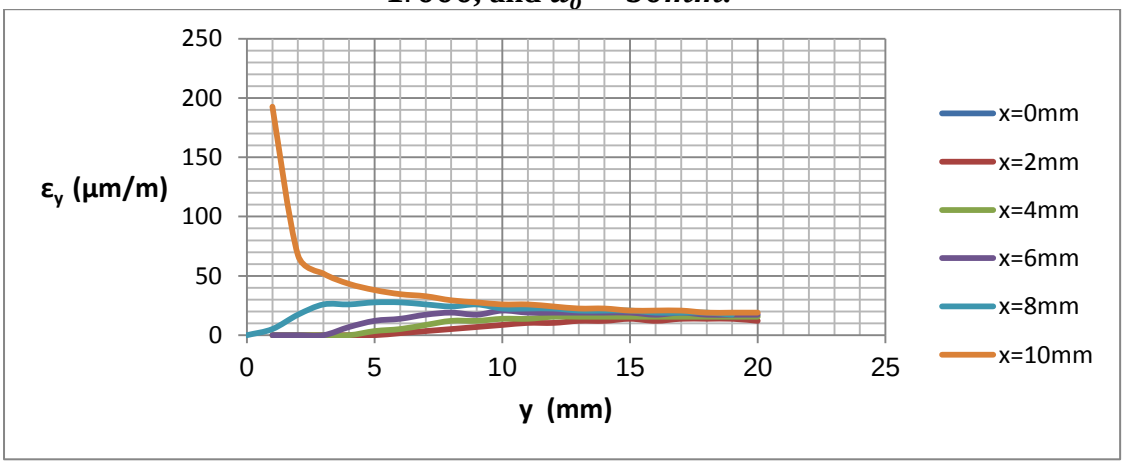


**Fig. (14) Nearby-Tip Strain Induced Towards the Y-axis for $Aspect\ Ratio = 1.000$, and $a_o = 30mm$.**

## 2. Failing-Strains Probability Distributions:

The probabilities by which the nearby-tip strains can cause total fracture for the cracked plates may be determined if the equation (14) should be obeyed. It has been shown previously, by examining the preceding subsection, that the lines on which the maximum strains $X$ and $Y$ are induced in thin plates are $y = 0$ and $x = 10$, respectively. One must therefore choose these lines under investigation in determining the failing-strain probabilities in order to thereby specify the points in which the maximum probabilities can appear, and also to investigate whatever point on which the total fracture may be evolved. Referring to Fig. (15) to Fig. (26), one can anticipate the facts that the failing strain probability distributions are independent of the crack length value change and also independent of the plate aspect ratio change, although the values of the maximum probabilities insignificantly fluctuate between 38-42% percent range, since these probabilities are of the same behavior regardless of how much the crack length and the aspect ratio would be. A further analysis may lead to the fact that the maximum probabilities always appear in the point in which the crack tip lies at, i.e., $X = 10$ and $Y = 0$. One can therefore conclude that the total fracture may start immediately as the crack grows starting from the right-hand crack tip **[4]**.

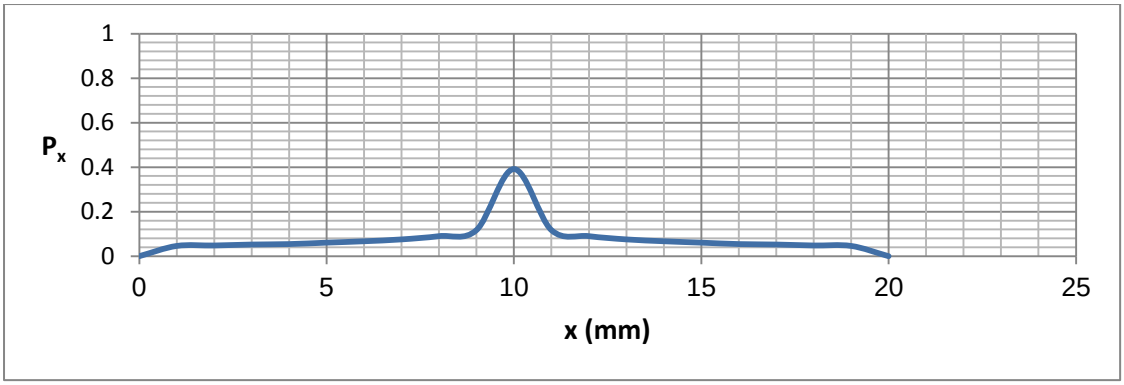


**Fig. (15) Failing-Strain Probability Distribution Along the X-axis for $y = 0mm$, $Aspect\ Ratio = 2.000$, and $a_o = 10mm$.**

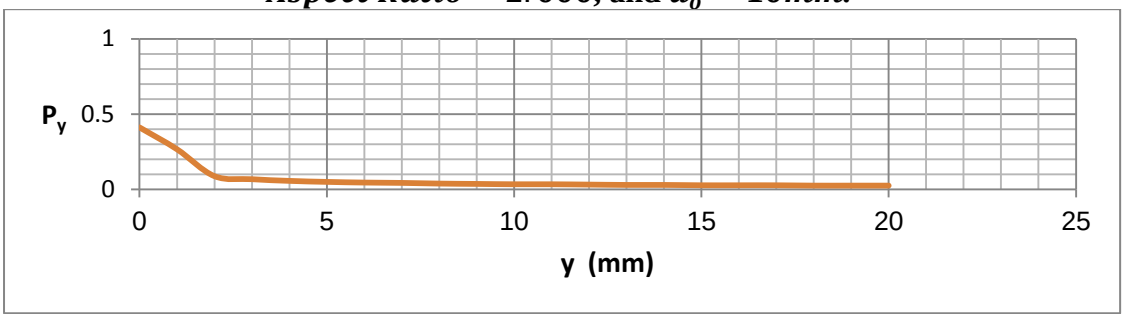


**Fig. (16) Failing-Strain Probability Distribution Along the Y-axis for $x = 10mm$, $Aspect\ Ratio = 2.000$, and $a_o = 10mm$.**

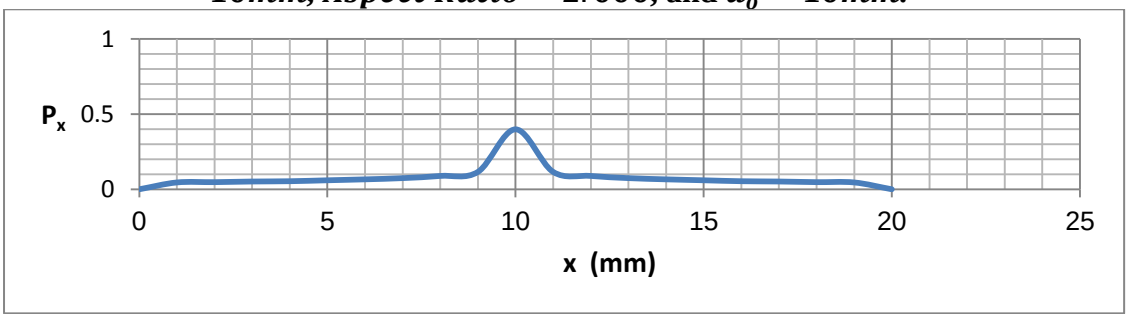


**Fig. (17) Failing-Strain Probability Distribution Along the X-axis for $y = 0mm$, $Aspect\ Ratio = 2.000$, and $a_o = 20mm$**

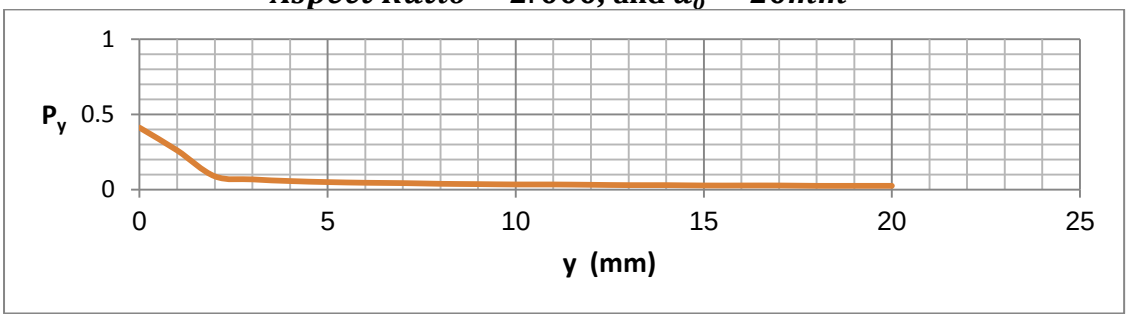


**Fig. (18) Failing-Strain Probability Distribution Along the Y-axis for $x = 10mm$, $Aspect\ Ratio = 2.000$, and $a_o = 20mm$.**

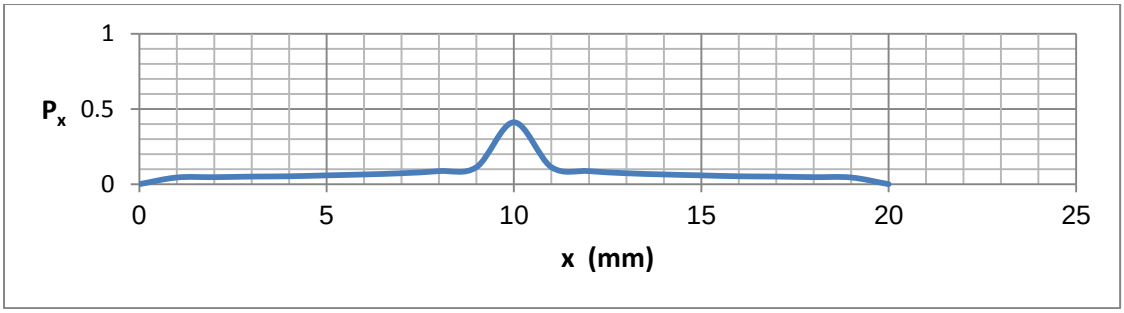


**Fig. (19) Failing-Strain Probability Distribution Along the X-axis for $y = 0mm$, $Aspect\ Ratio = 2.000$, and $a_o = 30mm$.**

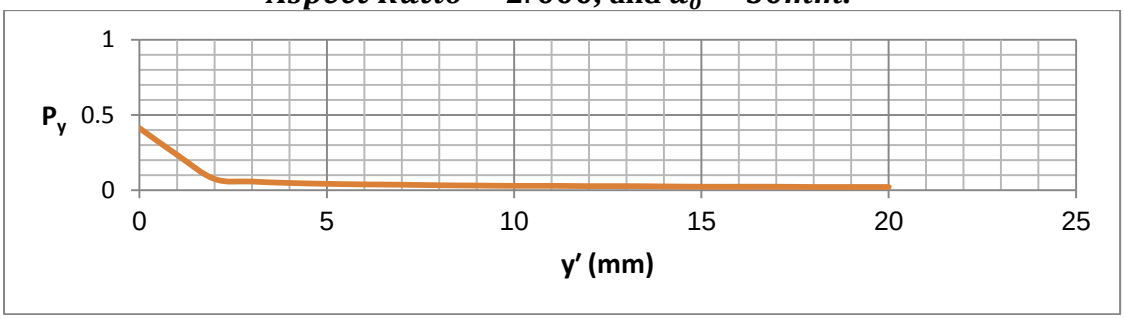


**Fig. (20) Failing-Strain Probability Distribution Along the Y-axis for $x = 10mm$, $Aspect\ Ratio = 2.000$, and $a_o = 30mm$.**

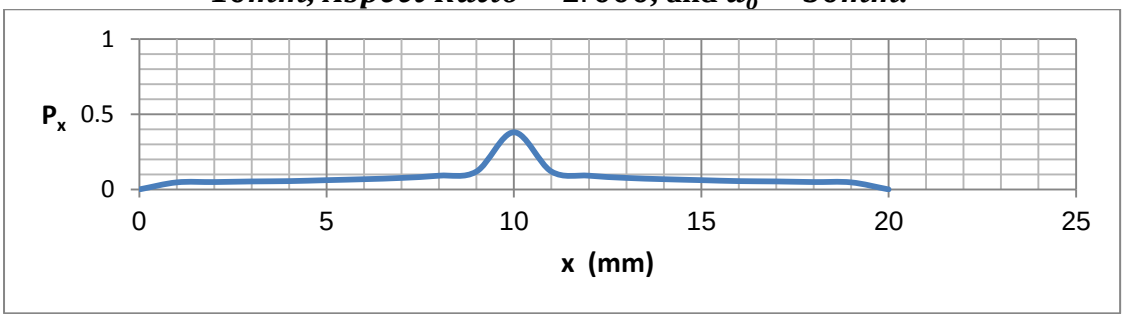


**Fig. (21) Failing-Strain Probability Distribution Along the X-axis for $y = 0mm$, $Aspect\ Ratio = 1.000$, and $a_o = 10mm$.**

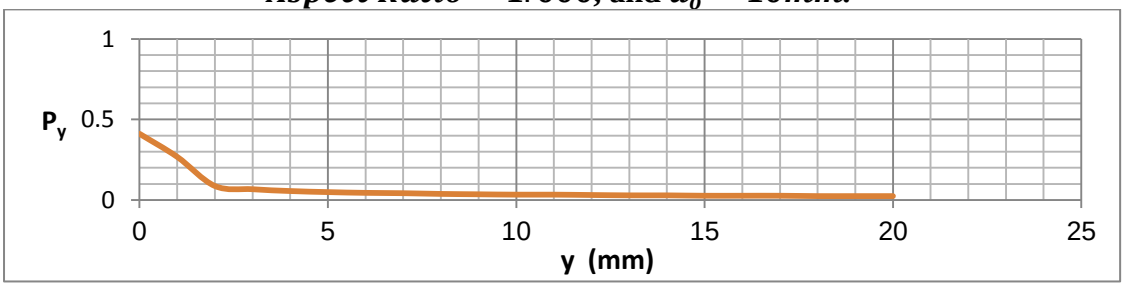


**Fig. (22) Failing-Strain Probability Distribution Along the Y-axis for $x = 10mm$, $Aspect\ Ratio = 1.000$, and $a_o = 10mm$.**

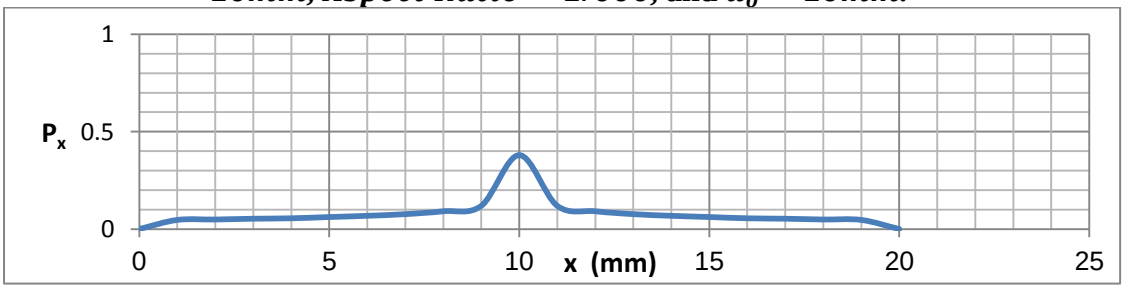


**Fig. (23) Failing-Strain Probability Distribution Along the X-axis for $y = 0mm$, $Aspect\ Ratio = 1.000$, and $a_o = 20mm$.**

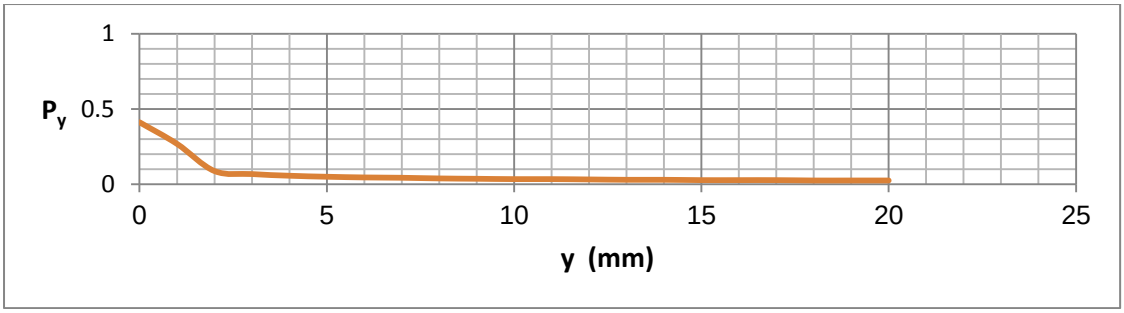


**Fig. (24) Failing-Strain Probability Distribution Along the Y-axis for $x = 10mm$, $Aspect\ Ratio = 1.000$, and $a_o = 20mm$.**

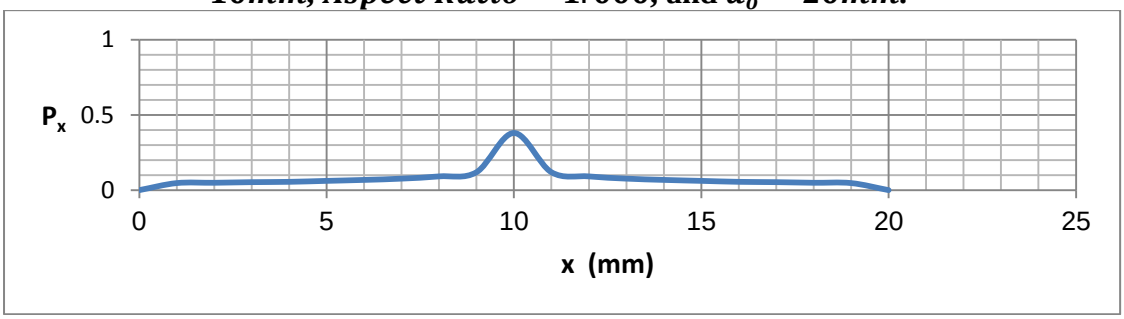


**Fig. (25) Failing-Strain Probability Distribution Along the X-axis for $y = 0mm$, $Aspect\ Ratio = 1.000$, and $a_o = 30mm$.**

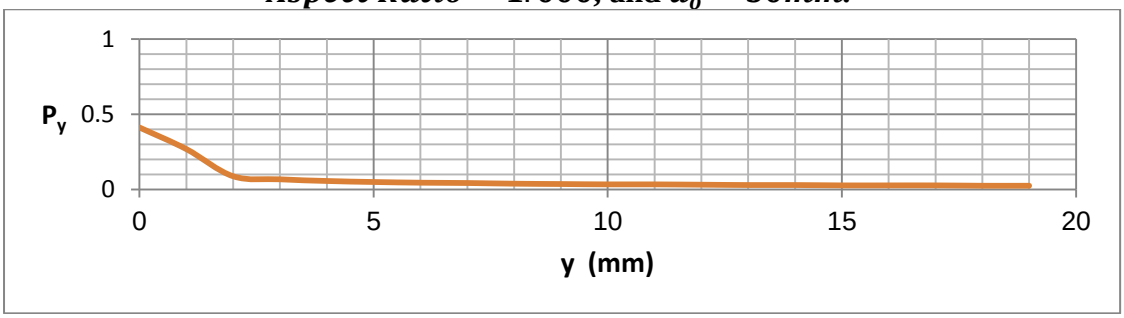


**Fig. (26) Failing-Strain Probability Distribution Along the Y-axis for $x = 10mm$, $Aspect\ Ratio = 1.000$, and $a_o = 30mm$.**

## References:


1. Kare Hellan. 1985. Introduction to Fracture Mechanics. University of Trondheim, Norway, Mc Graw Hill Book Company.
2. Muskhelishvili N. I. 1997. Some Basic Problems of the Fundamental Theory of Elasticity. Second Edition. Kluwer, The Language of Science.
3. Dugdale D. S. 2008. Yielding of Steel Sheets Containing Slits. J. Mech. Phys Sol., 8(2):100-104; Elsevier.
4. Ahmadi H. and Lotfollahi-Yaghin M. A. 2012. A probability distribution model for stress concentration factors in multi-planar tubular DKT-joints of steel offshore structures. J.AOR, 34(1):21-32, Elsevier.
5. Yevick D. 2003. Multicanonical Evaluation of Joint Probability Density Functions in Communication System Modeling. IEEE PhotonicsTechnology Center, 15(10).
6. Li Dong Ping, Li Xianmin, Gao Tianbao and Li Zheng. 2010. The Joint Distribution Effect on the Size Deformation Effect of Rock Mass. IEEE, 2:259-262.
7. Westergaard H. M. 1989. Bearing Pressures and Cracks. J. Applied Mechanics, 61:49-53.

**8.** Sedov L. I. 1992. A Course in Continuum Mechanics. Kluwer Academic Publishers.
**9.** Polmear I. J. 1995. Light Alloys: Metallurgy of Light Metals. Third Edition. Butterworth Heinmann.
**10.** Spiegel M. I., Schiller J. and Srinivasan R. A. 2009. Schaum Outlines of Probability and Statistics. Third Edition. Mc-Graw Hill Book Company.

# دراسة الانفعالات القريبة من حافة الشق واحتمالية حوث الفشل فيها للصفائح الرقيقة المعرضة لحمل صدمي وبمساعدة توزيعات الاحتمالية متعددة الاحداثيات المنقولة وذات متغيرين عشوائيين

**رشا عبد الحسين علي** **مثنى عبد الحسين علي***

جامعة بغداد – كلية التربية الرياضية الجادرية
*جامعة بغداد – كلية الهندسة – قسم الهندسة الميكانيكية

**الخلاصة:**
تعتبر احتمالية حصول الفشل في المقاطع والهياكل الهندسية الصلبة من احد مجالات الدراسة العلمية والهندسية المهمة في العديد من تطبيقاتها، ولهذا يعمد خبراء التصميم لايجاد النقاط التي تسبب فيها الانفعالات في فشل العينات المستخدمة وايجاد احتمالية وجود الانفعالات التي تسبب في انتشار الشقوق الموجودة في العينات المستخدمة وايضا ايجاد الحلول التي يعتكد الخبراء التصميميين عليها للحد من انتشار هذه الشقوق.
سيتم التحري التحليلي في الدراسة الحالية عن الصفائح الرقيقة المثبتة تثبيتا بسيطا والتي تحوي علي شقوق سطحية ضمن تركيبها، وسيسبب الحمل الصدمي المسلط على هذه الصفائح في خلق انفعالات قد تكون لا متناهية في الكبر بالقرب من حافة الشق للشقوق الموجودة. وستكون توزيعات هذه الانفعالات واحتمالية افشالها للعينات المستخدمة ضمن المواضيع الاساسية التي يتطرق لها البحث الحالي.
سيتم استعمال طريقة محدثة للوصول الى المعادلات النهائية والتي تمثل الانفعالات القريبة من حافة الشق لعينات الالمنيوم النقي من نوع 1100 وذلك بالاستعانة بمفاهيم الصفائح الرقيقة التقليدية مع الاخذ بنظر الاعتبار تأثيرات الحمل الصدمي بالاضافة الى مفاهيم الكسر الميكانيكي. وسيتم ايضا اجراء دراسة احصائية بأستعمال التوزيعات الاحصائية متعددة الاحداثيات المنقولة لغرض استخدام متغيرين عشوائيين تم نقلهما لاحداثيات اكثر تلائما مع توزيع الانفعالات لغرض التحري عن التوزيعات الاحصائية المطلوبة لايجاد الفشل الحاصل في العينات المستخدمة بوجود الانفعالات المسلطة تسيطا نقطيا بالقرب من حافة الشق للشقوق الموجودة.

**الكلمات المفتاحية:** لتوزيعات الاحتمالية المشتركة، الدوال الاحتمالية متعددة القوانين، الانفعالات قرب حافة الشق، الصفائح الرقيقة، تحليلات الكسر والفشل